THE JOURNAL OF PHYSICAL CHEMISTRY B

Article

pubs.acs.org/JPCB

Electrostatic Interactions Govern "Odd/Even" Effects in Water-Induced Gemini Surfactant Self-Assembly

Sriteja Mantha,[†,§] Jesse G. McDaniel,[†,§] Dominic V. Perroni,[†] Mahesh K. Mahanthappa,[‡] and Arun Yethiraj*[,†]

[†]Department of Chemistry and Theoretical Chemistry Institute, University of Wisconsin−Madison, 1101 University Avenue, Madison, Wisconsin 53706, United States

[‡]Department of Chemical Engineering and Materials Science, University of Minnesota, 421 Washington Avenue, S.E., Minneapolis, Minnesota 55455, United States

Supporting Information

ABSTRACT: Gemini surfactants comprise two single-tailed surfactants connected by a linker at or near the hydrophilic headgroup. They display a variety of water-concentration-dependent lyotropic liquid crystal morphologies that are sensitive to surfactant molecular structure and the nature of the headgroups and counterions. Recently, an interesting dependence of the aqueous-phase behavior on the length of the linker has been discovered; odd-numbered linker length surfactants exhibit characteristically different phase diagrams than even-numbered linker surfactants. In this work, we investigate this "odd/even effect" using computer simulations, focusing on experimentally studied gemini dicarboxylates with Na^+ counterions, seven nonterminal carbon atoms in the tails, and either three, four, five, or six carbon atoms in the linker (denoted Na-73, Na-74, Na-75, and Na-76, respectively). We find that the relative electrostatic repulsion between headgroups in the different morphologies is correlated with the qualitative features of the experimental phase diagrams, predicting destabilization of hexagonal phases as the cylinders pack close together at low water content. Significant differences in the relative headgroup orientations of Na-74 and Na-76 compared to those of Na-73 and Na-75 surfactants lead to differences in linker−linker packing and long-range headgroup−headgroup electrostatic repulsion, which affects the delicate electrostatic balance between the hexagonal and gyroid phases. Much of the fundamental insight presented in this work is enabled by the ability to computationally construct and analyze metastable phases that are not observable in experiments.

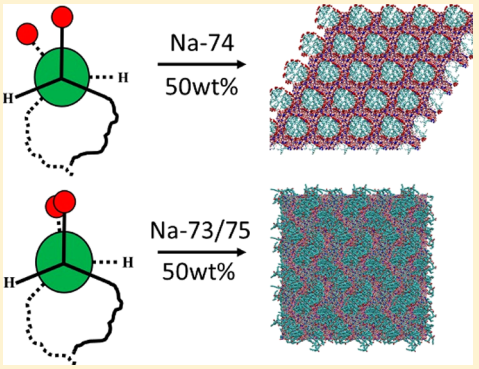

1. INTRODUCTION

Surfactant molecules can self-assemble in water to form aqueous lyotropic liquid crystalline (LLC) phases[1−4] with periodic, long-range nanoscale order. Examples include arrangements of spheres, hexagonally packed cylinders (hexagonal), and bicontinuous cubic (gyroid, double diamond, etc.) and lamellar morphologies. There has been recent interest in gemini surfactants,[5−10] which consist of two single-tailed surfactants connected by a linker (Figure 1), because they display bicontinuous morphologies over a wide range of concentrations. In addition to fundamental interest, these phases are of possible technological interest in the fabrication of membranes[11] with percolating water channels for selective chemical separations,[12−15] ion transport,[16] and controlled release formulations.[17,18]

The LLC phase diagram of gemini surfactant systems generally exhibits lamellar, gyroid, and hexagonal phases at low, intermediate, and high water content, respectively, but the relative stability regions (and even existence) of these phases depend on the type of headgroup and counterion, the length of the surfactant tail, and the position of the linker.[9,19−21] Gin and co-workers reported that cationic gemini surfactants employing quaternary ammonium,[12] phosphonium,[22,23] and imidazolium[24]

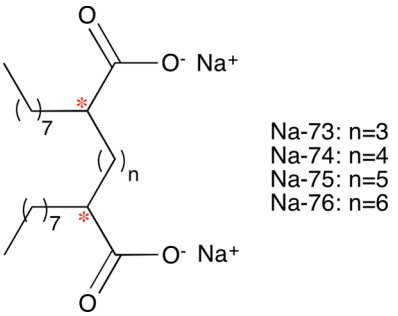

Figure 1. Schematic representation of the gemini surfactant molecules. Carbon atoms marked in red are chiral; we consider only "RR" chirality (see the Methods section).

Received: July 9, 2016
Revised: December 23, 2016
Published: December 27, 2016

Downloaded via CALIFORNIA INST OF TECHNOLOGY on September 3, 2023 at 20:20:17 (UTC).
See https://pubs.acs.org/sharingguidelines for options on how to legitimately share published articles.

© 2016 American Chemical Society

DOI: 10.1021/acs.jpcb.6b06882
J. Phys. Chem. B 2017, 121, 565−576

headgroups exhibit a slightly greater tendency to form the gyroid morphology than the corresponding single-chain surfactant molecules. Sorenson et al. showed that (anionic) dicarboxylate gemini surfactants exhibit a strong propensity to form gyroid morphologies over wide concentration and temperature ranges.[9] From computer simulations of dicarboxylate surfactants, Mondal et al.[25] proposed that reducing the electrostatic attraction between the headgroup and counterion (i.e., going from Na^+ to tetramethylammonium counterion) destabilizes lamellae compared with the gyroid.

Complementary micellization studies have additionally illuminated the interesting physics of gemini surfactant systems. While gemini surfactants generally exhibit critical micelle concentrations (CMCs) that are 1−2 orders of magnitude lower than those of the corresponding single-tail surfactants,[8] the linker length dependence can vary qualitatively with surfactant; the CMC may monotonically increase with the linker length,[26,27] show oscillatory behavior,[28] or exhibit either intermediate minima[29] or maxima.[30] In general, the CMC decreases monotonically with increasing tail length;[31−34] however, such trends are not always conserved for other properties. For example, Li et al.[32] reported an odd/even trend in the enthalpy of micellization with tail length despite the monotonic CMC dependence; the enthalpy of micellization was generally negative and decreasing with tail length for even-numbered but positive and increasing with tail length for odd-numbered carbon tails. A different odd/even trend, this time with the number of linker carbon atoms, was found for the ellipticity of gemini-surfactant-based mixed micelles.[35] These odd/even trends have been rationalized as manifestations of the "alternating polarity" or "donor−acceptor" theory that is used to explain similar trends found for nonionic hydrocarbon systems[36−38] and single-chain-surfactant-based emulsions.[39]

Mahanthappa and co-workers[9,10] have recently discovered that the dicarboxylate gemini surfactants with an odd number of carbon atoms in the linker (n = 3 and 5, see Figure 1) do not form the hexagonal LLC phase that is seen in surfactants with an even number (n = 4 and 6) of linker atoms at high water content. The origin of this surprising difference in phase behavior was unclear, although it was speculated that the linker conformation differences might affect the packing of the tails in different morphologies. In this work, we will argue that these odd/even phase behavior differences are not due to the alternating polarity effects, which have been the basis for the explanation of the previously reported odd/even trends, but rather are caused by a very different physical mechanism.

Using molecular dynamics (MD) simulations, we construct regular-hexagonal and gyroid-like LLCs composed of the Na-73, Na-74, Na-75, and Na-76 dicarboxylate gemini surfactants that were studied by Mahanthappa and co-workers;[9,10] notably, some of the investigated morphologies are metastable and are not seen experimentally. This enables a direct comparison of the structure and energetics of each morphology for the four different surfactants, illuminating the fundamental physics dictating the phase behavior. From this analysis, we find important differences in the electrostatic properties of the hexagonal and gyroid phases that sensitively depend on the hydration level. At higher water content, hexagonal phases exhibit lower headgroup repulsion due to their high interfacial curvature, whereas at lower water content the headgroup repulsion is higher than that in the gyroid phase due to the unfavorable close packing of cylinders. These trends are analogously reflected in the relative pairwise correlations between headgroups and counterions, with greater correlation for systems requiring greater headgroup screening. We show that there is a clear odd/even trend in the headgroup repulsion for the hexagonal phase at lower water content; this is due to the intercylinder headgroup repulsion, which is relatively higher for the odd surfactants because their intrinsic conformations orient the headgroups normal to the interface. Our work thus provides a qualitative explanation for the previously reported experimental odd/even trends in the phase behavior of dicarboxylate gemini surfactants; however, quantitative prediction of the relative phase stability requires additional characterization of long-range fluctuations in the hexagonal phase.

This article is organized as follows. After characterizing the LLC phases by their scattering structure factors, we examine the differences in the headgroup orientation and packing of the different surfactants; these differences are conserved across the phase diagram and are inherent to the intrinsic conformational preferences of the surfactants. We then analyze the ion−ion correlations and energetics of the surfactant morphologies. To establish general trends, we study the hexagonal and gyroid morphologies at three different hydration levels for each of the four different surfactants. We consider the hydration levels of λ = 12.9, 15, and 24.4, where λ denotes the number of water molecules per surfactant. We note that these hydration levels roughly span the experimental stability region of both the hexagonal and gyroid phases for Na-74 surfactants.[9]

2. METHODS

MD simulations are conducted at 300 K and 1 bar utilizing the GROMACS simulation package.[40] The GROMOS45a3 united atom force field[41] is employed for the surfactant molecules and Na^+ counterions, and the SPC model[42] is used for water. Equilibration in the NPT ensemble is run for ∼1 μs using a time step of 4 fs. Lennard-Jones interactions are switched to zero at 1.4 nm, and the particle-mesh Ewald method[43] is used for electrostatics. The water molecules are kept rigid using the SETTLE algorithm.[44] Isotropic and semi-isotropic pressure couplings are used for the gyroid and hexagonal phases, respectively, using the Berendsen barostat.[45] It is important to note that the gemini surfactants contain two chiral carbon centers, potentially resulting in three possible stereoisomers (RR, RS, and SS) for each surfactant; in this work, for simplicity, we consider only the RR surfactants.

It is imperative to consider the initial choice of the simulation box, as this determines the morphology of the equilibrated phase. This is because in the NPT ensemble, with a constant number of molecules, the density and unit cell dimensions are coupled. Because the energy depends strongly on the system density and only weakly on the unit cell dimensions, the initial choice of the number of molecules determines the resulting unit cell dimensions through optimization of the density. Therefore, it is impossible to *predict* either the unit cell dimensions or equilibrium LLC structure using NPT simulations without explicit free energy calculations; while this enables the study of metastable phases through constraining the size/shape of the simulation box, it also means that unit cell parameters for these phases must be predetermined. Our choice of initial unit cell dimensions is largely based on the experimentally determined values[9,10] at the corresponding concentrations. For the metastable phases, the unit cell dimensions are taken to be the same as those of the corresponding experimentally observed phases formed by the

DOI: 10.1021/acs.jpcb.6b06882
J. Phys. Chem. B 2017, 121, 565−576

other surfactants. We note that the gyroid systems at 65 wt % have slightly smaller unit cells compared to those in the experiment; these are chosen to be consistent with the Na-74 gyroid structure taken from Mondal et al.[25] The number of molecules and unit cell dimensions for each system are given in Table 1; hydration levels of λ = 12.9, 15, and 24.4 correspond to surfactant weight fractions of 65, 62, and 50 wt %, respectively. Additional details concerning the system construction are given in the Supporting Information.

Table 1. Composition of Gemini Surfactant LLCs

surfactant	phase	λ	# surfactant	# ions	# water	unit cell[a]
Na-73	gyroid	12.9	250	500	3225	6.35
Na-74	gyroid	12.9	250	500	3225	6.40
Na-75	gyroid	12.9	250	500	3225	6.45
Na-76	gyroid	12.9	250	500	3225	6.51
Na-73	gyroid	15	250	500	3750	6.46
Na-74	gyroid	15	250	500	3750	6.51
Na-75	gyroid	15	250	500	3750	6.57
Na-76	gyroid	15	250	500	3750	6.63
Na-73	gyroid	24.4	225	450	5490	6.74
Na-74	gyroid	24.4	225	450	5490	6.76
Na-75	gyroid	24.4	225	450	5490	6.82
Na-76	gyroid	24.4	225	450	5490	6.87
Na-73	hex	12.9	24	48	310	3.15, 2.87
Na-74	hex	12.9	24	48	310	3.10, 3.01
Na-75	hex	12.9	24	48	310	3.01, 3.13
Na-76	hex	12.9	24	48	310	2.96, 3.51
Na-73	hex	15	24	48	360	3.16, 3.01
Na-74	hex	15	24	48	360	3.12, 3.17
Na-75	hex	15	24	48	360	3.13, 3.25
Na-76	hex	15	24	48	360	3.06, 3.44
Na-73	hex	24.4	24	48	586	3.29, 3.49
Na-74	hex	24.4	24	48	586	3.24, 3.65
Na-75	hex	24.4	24	48	586	3.22, 3.78
Na-76	hex	24.4	24	48	586	3.16, 3.99

[a]The unit cell of the gyroid is cubic and is specified by a single length (given in nm), whereas the unit cell of the hexagonal phase is specified by the magnitudes of "*a*" and "*b*" unit cell vectors (forming an angle of 120°) and the length of vector "*c*".

3. RESULTS AND DISCUSSION

3.1. Structure Factor Characterization of LLCs. Gyroid and hexagonal phases at λ = 12.9, 15, and 24.4 are constructed for Na-73, Na-74, Na-75, and Na-76 dicarboxylate gemini surfactants. While the formation of the hexagonal phase is clearly visualized, verifying the gyroid-phase formation is more difficult; the gyroid phase is rigorously characterized by its X-ray scattering pattern, with two high-intensity peaks corresponding to the (211) and (220) Bragg reflections and lower-amplitude peaks corresponding to the (321), (400), (420), and (332) reflections.[9,10] Figures 2 and 3 show computed scattering structure factors (see the Supporting Information for details) for all of the systems and the corresponding snapshots of both hexagonal and gyroid phases. While most are well-formed, exhibiting qualitatively similar scattering features with the corresponding experimental phases, the gyroid phases at λ = 24.4 are less perfect, exhibiting significant intensity scattering peaks that are not observed experimentally, most notably (200) and (210). However, these morphologies mostly show the characteristic scattering features of the gyroid phase, and so we consider these morphologies "gyroid-like". Because of the large number of systems studied, our analysis is not significantly limited by these gyroid-phase imperfections, as discussed in the Supporting Information.

3.2. Headgroup Orientation and Surfactant Packing. A major difference between the odd and even surfactant systems is the distribution of relative headgroup orientations characterized by the "dihedral" angle, ϕ (Figure 4). In the LLCs, the Na-73 and Na-75 surfactants exhibit a single peak at $\phi \sim -10°$, whereas the Na-74 and Na-76 surfactants exhibit a bimodal distribution with peaks at $\phi \sim \pm 40°$. These distributions are similar for both the hexagonal and gyroid phases (Figure 4) and are not significantly affected by hydration level (Figure S1). These different headgroup orientations are largely determined by the intramolecular, configurational surfactant energetics subject to the imposed general constraint that ϕ must be small ($-60° < \phi < 60°$) to allow surfactant packing in self-assembly. This is demonstrated by energetic analysis as well as additional simulations of the surfactants in bulk water. For surfactants in bulk water, the relative headgroup orientation of the surfactants (Figure S2) is qualitatively similar to that in the LLC morphologies for the range $-60° < \phi < 60°$. In Figure 5, the average configurational energy of the surfactants is plotted as a function of headgroup orientation (ϕ), and it is evident that the energetic minima directly correspond to the peaks in Figure 4. For surfactants in bulk water, additional minima exist for larger ϕ; however, such configurations are not permitted in the LLC phases due to packing restrictions. The intrinsic conformational differences of the odd and even gemini surfactants lead to differences in both surfactant packing (vide infra) and electrostatic interactions in the LLCs (Section 3.3), with the latter effect primarily responsible for the different odd/even phase behavior.

The odd/even surfactant conformational differences lead to differences in surfactant packing in the LLC morphologies. In Figure 6, the surfactant linker−linker center-of-mass radial distribution function (RDF) is plotted for the hexagonal and gyroid morphologies at λ = 15 for each of the four surfactants; RDFs at λ = 12.9 and 24.4 are shown in Figures S3 and S4, respectively. Clear trends exist, which only slightly depend on morphology: The Na-74 and Na-76 surfactants show closer linker−linker packing than either of the Na-73 or Na-75 surfactant; we attribute this to the conformational differences of the surfactants, as discussed earlier. These data do not imply a difference in the density of the surfactant packing but merely represent the relative "alignment" of neighboring surfactant molecules. Two important conclusions are drawn from these data: (1) the packing of a given surfactant is similar in both the hexagonal and gyroid phases (at similar water content) and (2) both the hexagonal and gyroid phases can accommodate the inherently different packing preferences of the four surfactants. Thus, the inherent configurational differences of the odd and even surfactants do not preclude the formation of either the hexagonal or gyroid phase on the basis of packing arguments alone. Relatedly, the specific morphology of the phase (hexagonal or gyroid) does not bias the surfactants to specific packing motifs, rather the packing seems to be predetermined on the basis of the inherent conformational properties of the specific surfactant. We note that the packing differences mainly pertain to the linker and headgroups of the surfactants, as there is little difference in the tail−tail packing, as shown in Figures 7, S5, and S6.

DOI: 10.1021/acs.jpcb.6b06882
J. Phys. Chem. B 2017, 121, 565−576

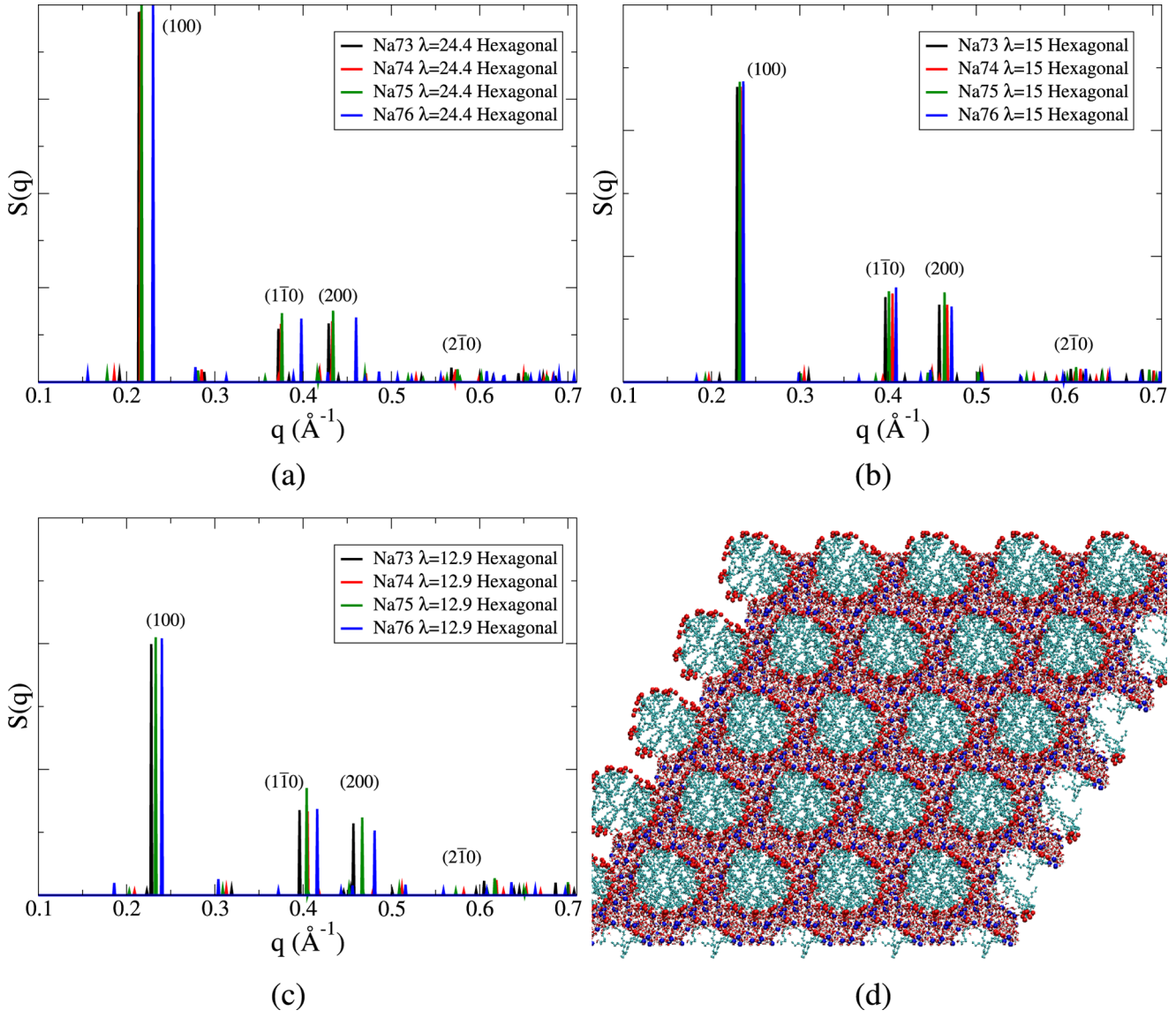

Figure 2. Structure factors of the hexagonal morphologies at (a) λ = 24.4, (b) λ = 15, and (c) λ = 12.9. (d) Representative simulation snapshot of Na-74 hexagonal morphology at λ = 24.4.

3.3. Ion Structure and Electrostatic Energetics. Because of the high density of free ions and ionic headgroups, electrostatic interactions are a dominant component of the cohesive energy in the gemini surfactant LLCs. These electrostatic interactions are strongly dependent on the hydration level due to two primary reasons: Water is a strong dielectric and effectively solvates both ionic headgroups and counterions, diminishing the correlation between these species at high hydration. Additionally, the hydration level determines the confinement length scales of the nanostructures such that the ionic groups are necessarily more proximal at low hydration levels. Below we demonstrate that the hydration dependence of these electrostatic interactions is different for the gyroid and hexagonal phases, which consequently affects the relative phase stability.

In Figure 8, we compare the RDFs between sodium counterions and the dicarboxylate headgroups for the hexagonal and gyroid phases at the two extreme hydration levels, λ = 12.9 and 24.4. While we specifically focus on the Na-74 surfactant systems for brevity, the qualitative conclusions are the same for all other surfactants (Figures S9 and S10). The hydration dependence of the headgroup−counterion correlation is significantly different for the gyroid and hexagonal phases; the height of the first RDF peak increases by a factor of ∼2.4 for the hexagonal phase but only by ∼1.6 for the gyroid phase, as the hydration level is decreased from λ = 24.4 to 12.9. These differences in counterion screening reflect the relative electrostatic repulsion between headgroups in the different morphologies. At high hydration, there is lower headgroup repulsion in the hexagonal phase due to the high curvature of the cylinders; however, at lower hydration, the cylinders in the hexagonal phase pack closer together, resulting in high intercylinder electrostatic repulsion and higher counterion screening than in the gyroid phase. It is important to point out that these hydration levels approximately span the experimental stability transition between the Na-74 hexagonal and gyroid phases,[9] with the hexagonal and gyroid phases experimentally observed at λ = 24.4 and 12.9, respectively. The crossover in the relative headgroup−counterion correlation between the hexagonal and gyroid phases in Figure 8 thus qualitatively

DOI: 10.1021/acs.jpcb.6b06882
J. Phys. Chem. B 2017, 121, 565−576

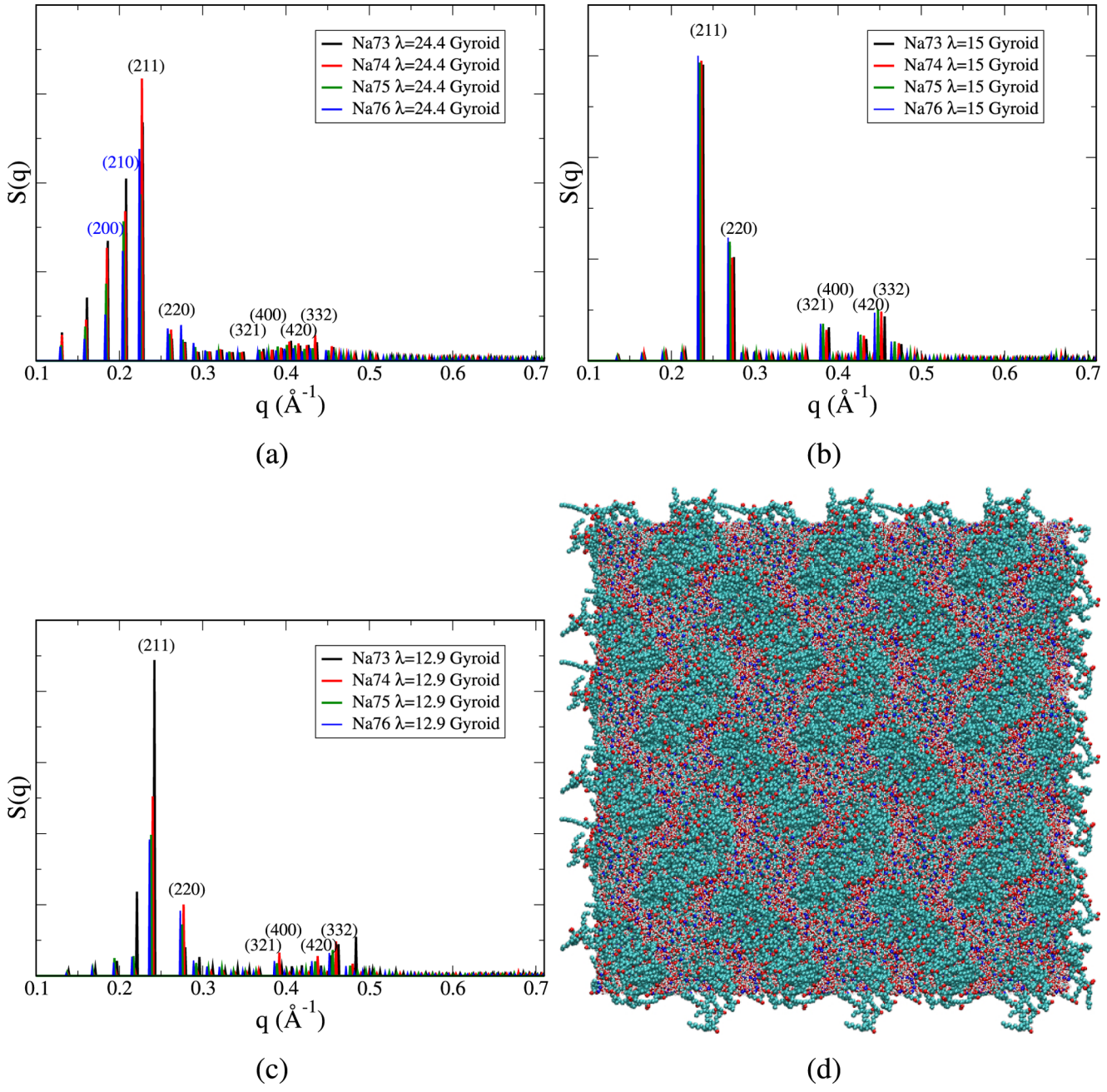

Figure 3. Structure factors of the gyroid morphologies at (a) λ = 24.4, (b) λ = 15, and (c) λ = 12.9. (d) Representative simulation snapshot of Na-74 gyroid morphology at λ = 12.9 from the (100) perspective.

mirrors the crossover in experimental stability; this is not a predictive measure, however, as similar qualitative trends are seen for the Na-73 and Na-75 surfactants (Figures S9 and S10), which do not experimentally exhibit a hexagonal phase.

To examine the surfactant dependence of the electrostatic properties, an initial consideration is the spatial correlation of the dicarboxylate headgroups in the LLCs, as increasing the linker length directly results in a greater separation of the two headgroups on each surfactant. In Figure 9, we compare headgroup−headgroup RDFs for λ = 15 hexagonal and gyroid phases for the four different surfactants; these RDFs include both intra- and inter-surfactant headgroup correlations. In general, all of the surfactants show similar headgroup correlation structure, with longer linker surfactants exhibiting stronger correlation at longer separations and weaker correlation at shorter separations. The obvious outlier is the Na-73 system, in which the headgroup−headgroup correlation is significantly enhanced at approximately 4−5 Å distances, which is due to the short linker and the resulting intrasurfactant correlation. However, the longer linker surfactants also exhibit approximately 4−5 Å peaks, indicating significant intersurfactant correlation at these separations. We note that the close intrasurfactant headgroup−headgroup correlation for Na-73 is independent of morphology and does not seem to directly affect the headgroup−counterion correlation (Figure 10), as discussed below.

We next examine how the headgroup−counterion correlation in the hexagonal and gyroid morphologies is affected by the surfactant linker length. In Figure 10, the corresponding RDFs are shown for the hexagonal and gyroid phases of the four

DOI: 10.1021/acs.jpcb.6b06882
J. Phys. Chem. B 2017, 121, 565−576

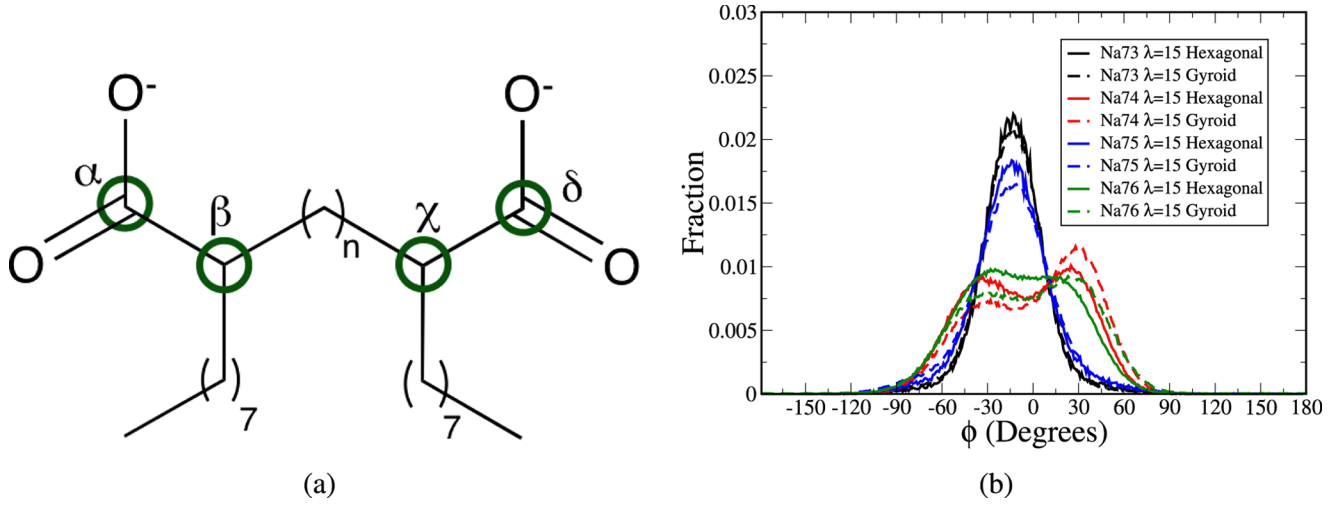

Figure 4. (a) Relative headgroup orientation (ϕ) defined by the dihedral angle formed by planes of $\alpha-\beta-\chi$ and $\beta-\chi-\delta$ atoms and (b) ϕ distribution of surfactant molecules for λ = 15 morphologies.

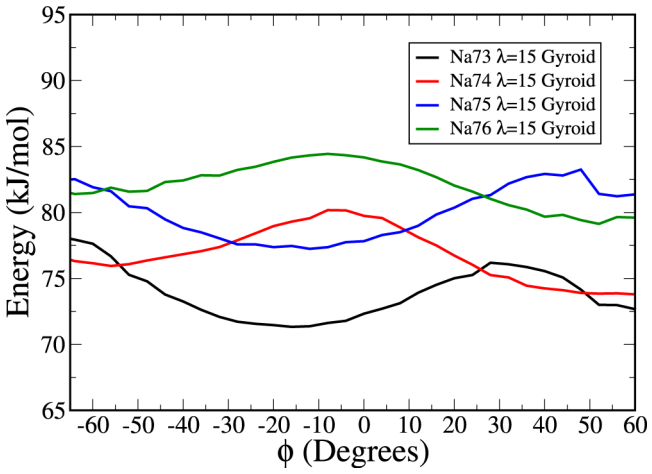

Figure 5. Conformational energy of surfactant molecules as a function of their headgroup orientation (ϕ). Note that we exclude the intramolecular electrostatic interaction contributions, as these are characterized elsewhere (Figure 11).

different surfactants at hydration λ = 15. We note that the qualitative trends are similar at the other hydration levels (Figures S9 and S10) although the analysis is somewhat complicated by imperfections in the gyroid structure. The gyroid phase exhibits monotonically increasing headgroup−counterion correlation as the linker length is increased. The hexagonal phase interestingly exhibits monotonic behavior that is grouped within the distinct odd/even sets, as is clearly illustrated by plotting the intensity of the first RDF peak as a function of linker length (Figure 10c). The general monotonic trends are due to the greater confinement of the hydrophilic water channels as the linker length is increased, the latter being inferred from the unit cell dimensions in Table 1. The cylinders pack closer together in the hexagonal phase (smaller a, b vectors) with increasing linker length, and the gyroid unit cell size increases, implying sharper interfaces (fixed number of water molecules). It has previously been shown that the headgroup−counterion correlation is extremely sensitive to the confinement length scale and increases with narrower confinement.[25,46]

What then explains the odd/even grouping of headgroup−counterion correlation in the hexagonal phase? As shown in Figure 10c, the correlation increases similarly with length for the odd and even linker surfactants but is relatively lower for even surfactants. We propose that this odd/even shift in the

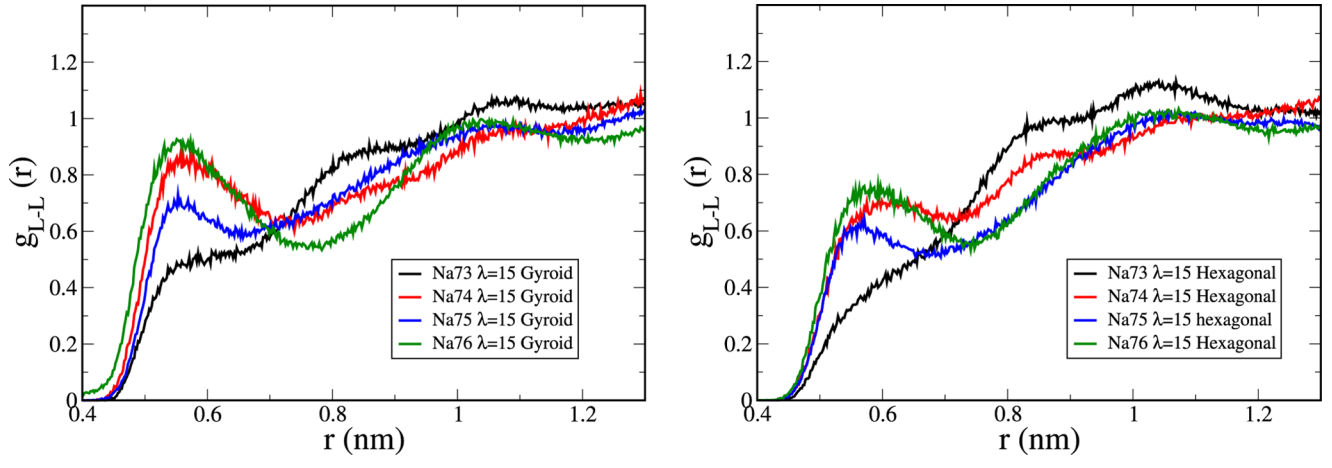

Figure 6. Surfactant linker−linker center-of-mass RDFs for the (left) gyroid and (right) hexagonal phases at λ = 15.

DOI: 10.1021/acs.jpcb.6b06882
J. Phys. Chem. B 2017, 121, 565−576

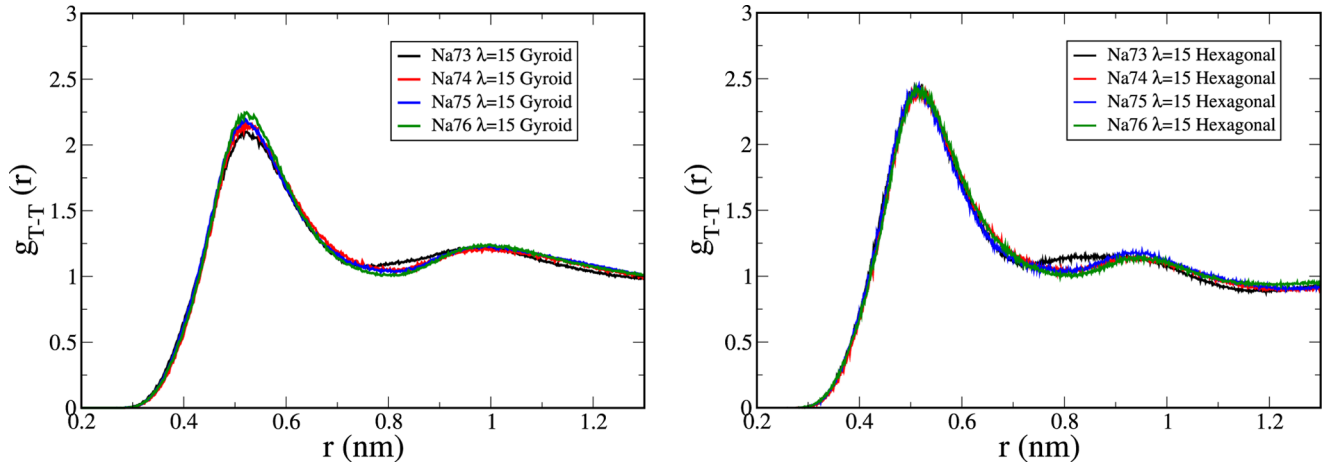

Figure 7. Surfactant tail−tail center-of-mass RDFs for the (left) gyroid and (right) hexagonal phases at λ = 15.

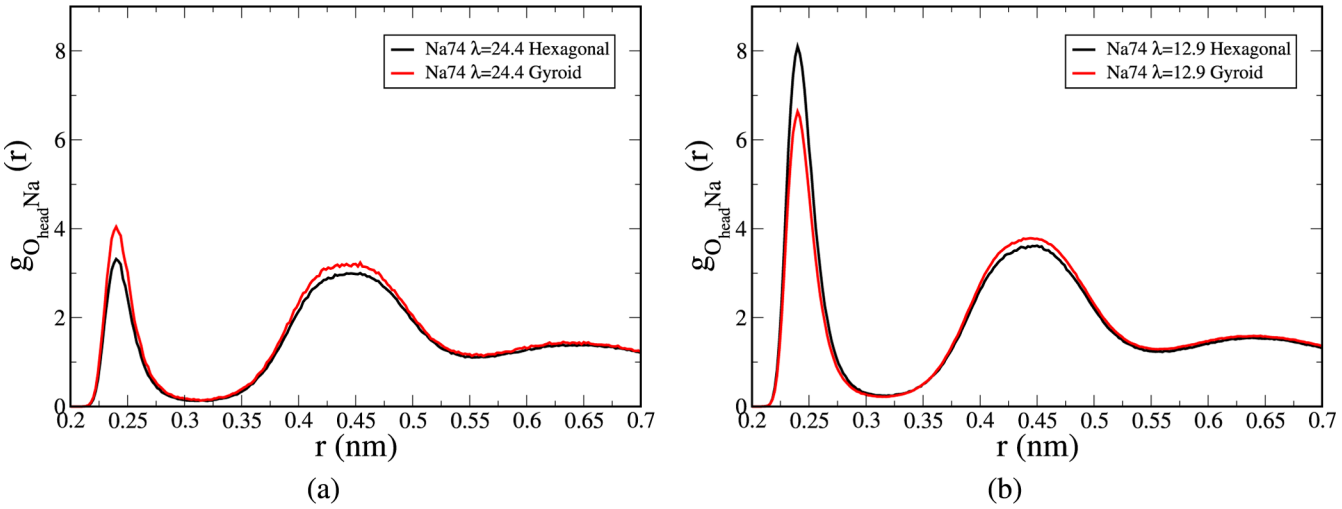

Figure 8. Comparison of RDFs between dicarboxylate oxygen atoms and sodium counterions for hexagonal and gyroid phases of Na-74 surfactants at hydration levels (a) λ = 24.4 and (b) λ = 12.9.

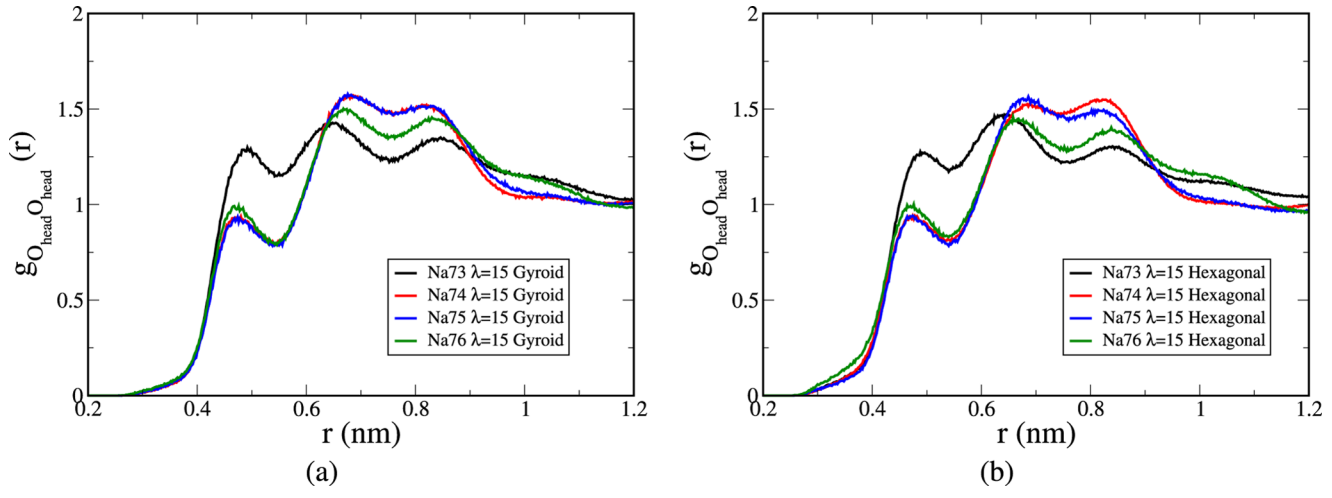

Figure 9. RDFs between dicarboxylate oxygen atoms at λ = 15 for (a) gyroid phases and (b) hexagonal phases.

counterion screening is due to differences in the intercylinder headgroup repulsion in the hexagonal phases. To demonstrate this, we calculate the electrostatic energy of the dicarboxylate headgroups in a uniform, compensating background charge; this is a common practical approach for describing the energetics of infinite, charged systems (see the Supporting Information for details). In Figure 11, we plot this electrostatic energy for the hexagonal phases of the four different surfactants at the three different hydration levels. Trends in the headgroup repulsion are inferred from these energy densities; more

DOI: 10.1021/acs.jpcb.6b06882
J. Phys. Chem. B 2017, 121, 565−576

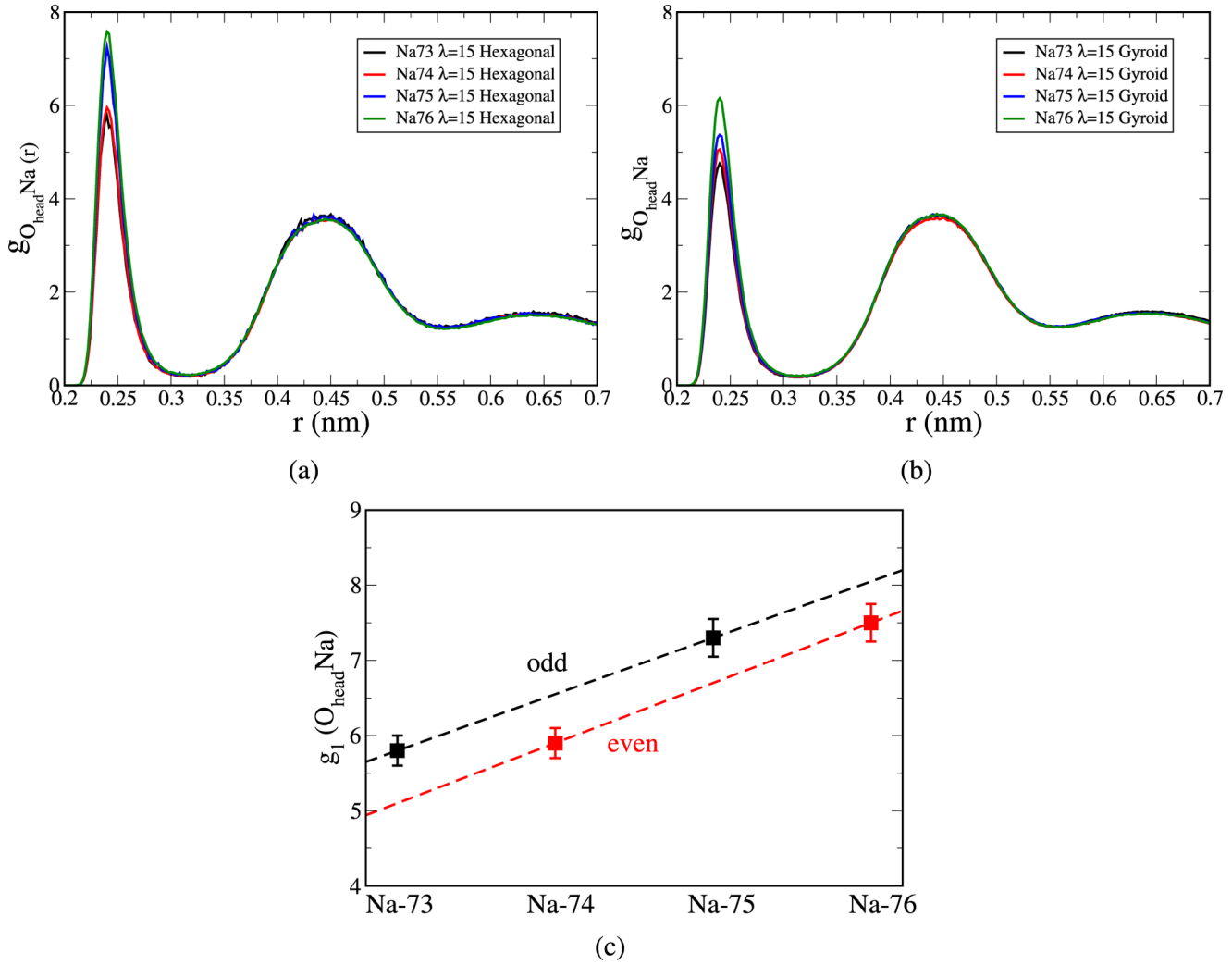

Figure 10. RDFs between carboxylate oxygen atoms and sodium counterions for (a) hexagonal phases and (b) gyroid phases at the λ = 15 hydration level. (c) Height of the first peak in the RDF for the hexagonal phases.

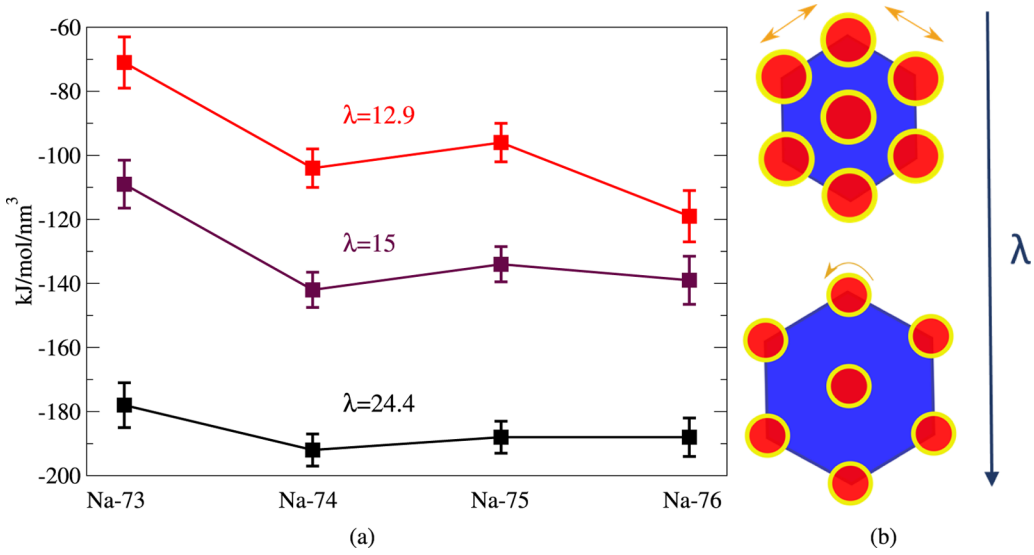

Figure 11. (a) Electrostatic energy of dicarboxylate headgroups in uniform background charge for hexagonal morphologies at different hydration levels. (b) Schematic depiction of intra- and inter-cylinder repulsion in hexagonal phases at different hydration levels.

negative values imply lower headgroup repulsion and vice versa. These energies are very sensitive to the ion density, with less negative energies (greater repulsion) for smaller confinement (smaller λ). Also, the electrostatic headgroup repulsion for the

DOI: 10.1021/acs.jpcb.6b06882
J. Phys. Chem. B 2017, 121, 565−576

Na-73 phases is comparatively high, which we attribute to the short intrasurfactant headgroup correlation distance (Figure 9). At low hydration (λ = 12.9), the cylinders in the hexagonal phase are much more closely packed and there is an odd/even trend, in which the even surfactants generally exhibit lower headgroup repulsion (more negative energies) than the odd surfactants. The fact that this odd/even trend becomes prominent with smaller confinement suggests that it reflects the differences in the intercylinder repulsion within the hexagonal phases. We believe that these differences are due to the orientation of the headgroups of odd surfactants more normal to the cylinder surface because of their relative headgroup orientation (Figure 4). The odd/even dependence of the counterion screening in the hexagonal phase (Figure 10) is thus caused by these differences in electrostatic repulsion between the close-packed cylinders.

Our combined analysis of the headgroup−counterion correlation (Figures 8 and 10) and electrostatic headgroup repulsion (Figure 11) suggests that the preferential formation of hexagonal or gyroid phase is due to the hydration-dependent balance of the electrostatic interactions between the headgroups and counterions. Although the balance of ionic attractions and repulsions is obviously a general phenomenon, it is important to realize that in these systems there is a clear cause and effect: the headgroup−headgroup repulsion is predetermined on the basis of the phase topology, and the counterions provide the requisite screening. We note that none of the mentioned morphologies or odd/even trends exist in the headgroup−water RDF (Figures S11, S12, and S13). The nearly exact quantitative balance of attraction, repulsion, and screening of the headgroups, counterions, and water in the hexagonal and gyroid phases (for a given λ) is demonstrated by the average total electrostatic energies in Tables 2−4. The

Table 2. Energy Density of Gyroid and Hexagonal Phases at λ = 24.4[a]

	electrostatic energy (kJ/mol nm^3)		total potential energy (kJ/mol nm^3)	
system	gyroid	hexagonal	gyroid	hexagonal
Na-73	−2133	−2129	−1969	−1963
Na-74	−2106	−2097	−1950	−1940
Na-75	−2050	−2044	−1897	−1889
Na-76	−2004	−2003	−1855	−1853

[a]The uncertainty in the energies is at least 2−3% due to fluctuations of the hexagonal phase and imperfections in the gyroid structures.

Table 3. Energy Density of Gyroid and Hexagonal Phases at λ = 15[a]

	electrostatic energy (kJ/mol nm^3)		total potential energy (kJ/mol nm^3)	
system	gyroid	hexagonal	gyroid	hexagonal
Na-73	−2259	−2251	−2112	−2104
Na-74	−2208	−2191	−2068	−2051
Na-75	−2144	−2130	−2010	−1994
Na-76	−2086	−2079	−1957	−1950

[a]The uncertainty in the energies is at least 2−3% due to fluctuations of the hexagonal phase and imperfections in the gyroid structures.

gyroid and hexagonal phases exhibit similar electrostatic and total energies at all three hydration levels and for all four surfactant molecules. For a specific morphology, the energy

Table 4. Energy Density of Gyroid and Hexagonal Phases at λ = 12.9[a]

	electrostatic energy (kJ/mol nm^3)		total potential energy (kJ/mol nm^3)	
system	gyroid	hexagonal	gyroid	hexagonal
Na-73	−2274	−2277	−2134	−2136
Na-74	−2220	−2229	−2090	−2099
Na-75	−2166	−2152	−2038	−2025
Na-76	−2105	−2095	−1982	−1971

[a]The uncertainty in the energies is at least 2−3% due to fluctuations of the hexagonal phase and imperfections in the gyroid structures.

only slightly depends on the surfactant, with slightly less cohesive energy as the linker length increases. Additionally, the cohesive energy density for all systems increases with decreasing hydration because of the resulting greater ionic concentration. The energetic equivalence of the Na-74 and Na-76 hexagonal and gyroid phases at λ = 24.4 is not surprising; this is close to the experimentally observed stability transition region[9] for these systems. However, the near-equivalence in energy of the two phases for the Na-73 and Na-75 surfactants implies that the absence of experimentally observed hexagonal phases for the odd linker−surfactant systems[10] is due to very subtle physics, potentially long-range fluctuations (vide infra), or entropic differences resulting from the relative ion correlation. The uncertainty in the energy values reported in Tables 2−4 is at least 2−3% due to fluctuations of the hexagonal phase and imperfections in the gyroid structures.

We finally comment on an important discrepancy related to long-range fluctuations between our ideal, simulated LLC morphologies and the corresponding experimental systems. Both experimental[47−49] and theoretical[50,51] work have demonstrated the importance of long-range fluctuations in these and similar morphologies formed by diblock copolymers or phospholipid bilayers. In particular, these fluctuations become increasingly important near stability transitions and may mediate the transition between morphologies.[47] In the present case, the neglect of such fluctuations is presumably more problematic for the hexagonal phase, as the gyroid has a significantly larger unit cell and is more structurally rigid because of its 3D network connectivity. Indeed, the X-ray diffraction spectrum of the experimental Na-74 hexagonal phase shows no sharp (200) peak,[9] in contrast to our simulated hexagonal phase, indicating some degree of long-range disorder in the experimental system. To examine the qualitative effects of fluctuations, we conducted additional simulations of 2 × 2 × 2 supercells of the hexagonal morphologies (note "supercell" is somewhat arbitrary, as the hexagonal phase is only 2D periodic, but is defined relative to the systems in Table 1). Simulations employing supercells generally exhibited increased headgroup repulsion and headgroup−counterion correlation, both with average enhancements of roughly 5% compared to those of the unit cell simulations. This indicates that fluctuations in the hexagonal morphology generally result in larger electrostatic interactions than those in the ideal LLC structures, with quantitative predictions requiring incorporation of these effects.

4. CONCLUSIONS

Our simulations suggest that the linker-dependent phase behavior of dicarboxylate gemini surfactant LLCs is largely due to a subtle balance of the electrostatic interactions between the headgroups and counterions. At high hydration levels, the

DOI: 10.1021/acs.jpcb.6b06882
J. Phys. Chem. B 2017, 121, 565−576

high curvature of the cylinders in the hexagonal morphologies leads to lower headgroup−headgroup repulsion than in the gyroid phase; however, as the water content decreases, the trend is reversed due to high intercylinder repulsion in the hexagonal phase. However, these electrostatic differences are largely balanced by the attraction and screening of the Na^+ counterions, resulting in near-equivalency of the total electrostatic energy of the hexagonal and gyroid phases. This delicate energetic balance makes the phase behavior highly sensitive to the specific surfactant, counterion, and temperature.[9,10]

Different surfactants (e.g., Na-73, Na-74, Na-75, and Na-76) or counterions (e.g., Na^+ and K^+) may modulate the phase behavior by altering this electrostatic balance.[52−54] The linker-dependent phase behavior of gemini surfactants is due to the differences in the headgroup−headgroup repulsion caused by inherent conformational preferences of the surfactants. Relatedly, we expect that the equilibrium between the hexagonal and gyroid phases may be shifted with a different choice of counterion; a more weakly interacting counterion (e.g., tetramethylammonium (TMA^+)) may alter the hydration-dependent electrostatic balance between morphologies, changing the phase diagram. Our analysis is consistent with previous mechanistic studies[25] of the phase behavior of gemini surfactant systems. For example, Mondal et al.[25] observed that a low-water-content lamellar phase of Na-74 dicarboxylate surfactants was destabilized with respect to the gyroid phase when Na^+ counterions were replaced by TMA^+. These authors speculated that the relative stability of the two phases was electrostatic in nature and the stability of the lamellar phase required strong counterion correlation. Indeed, because of the absence of curvature in the lamellar phase, one expects greater headgroup−headgroup repulsion than in the gyroid phase, requiring greater counterion screening.

We finally speculate on the qualitative differences in the experimental phase diagrams of even (Na-74, Na-76) and odd (Na-73, Na-75) dicarboxylate surfactant systems.[9,10] By ruling out other explanations, our simulations suggest that the absence of experimental hexagonal phases for the Na-73 and Na-75 surfactants may be caused by long length scale fluctuations from ideal LLC structure. For example, the single unit cell hexagonal phases in our simulations consist of perfectly packed, infinitely "straight" cylinders; such ideal systems are mechanically unstable and do not incorporate long length scale fluctuations in either the cylinder curvature or cylinder packing. By employing supercell simulations, we have shown that deviations from ideal cylindrical packing enhance the electrostatic interactions, including repulsion between cylinders, and counterion correlation. Thus, the reduced intercylinder repulsion and the lower counterion correlation of the Na-74 and Na-76 surfactants may allow for enhanced stabilization of long-range curvature fluctuations and packing defects of the hexagonally packed cylinders; the odd surfactant (Na-73, Na-75) hexagonal phases will be more destabilized by imperfect packing because of the higher intercylinder headgroup repulsion. Theoretical verification of this requires the ability to model long length scale fluctuations over numerous unit cells, which may be achieved by utilizing field theories similar to those developed in the diblock copolymer community.[51]

■ ASSOCIATED CONTENT

Supporting Information

The Supporting Information is available free of charge on the ACS Publications website at DOI: 10.1021/acs.jpcb.6b06882.

Further computational details concerning construction of systems and self-assembly, details of structure factor calculations, relative headgroup orientation for λ = 12.9 and 24.4 systems, configurations of single gemini surfactant molecules in bulk water, linker−linker RDFs for λ = 12.9 and 24.4 systems, tail−tail RDFs for λ = 12.9 and 24.4 systems, headgroup−headgroup RDFs for λ = 12.9 and 24.4 systems, headgroup−counterion RDFs for λ = 12.9 and 24.4 systems, water−headgroup RDFs for all systems, and discussion of calculating the electrostatic energy of charged systems (PDF)

■ AUTHOR INFORMATION

Corresponding Author

*E-mail: yethiraj@chem.wisc.edu.

ORCID

Arun Yethiraj: 0000-0002-8579-449X

Author Contributions

§S.M. and J.G.M. contributed equally to this work.

Notes

The authors declare no competing financial interest.

■ ACKNOWLEDGMENTS

This work was supported by the Department of Energy under award number DE-SC0010328. We acknowledge computational support through Extreme Science and Engineering Discovery Environment (XSEDE) allocations under grant number TG-CHE090065. We acknowledge support from the UW-Madison Chemistry Department cluster under grant number CHE-0840494 and computational resources and assistance of the UW-Madison Center for High Throughput Computing (CHTC). We thank Dr. Jagannath Mondal for sharing with us different input files for setting up initial simulations.

■ REFERENCES

(1) Hyde, S. In *Handbook of Applied Surface and Colloid Chemistry*; Holmberg, K., Ed.; Wiley: New York, 2001; pp 299−332.

(2) Kato, T.; Mizoshita, N.; Kishimoto, K. Functional Liquid-Crystalline Assemblies: Self-Organized Soft Materials. *Angew. Chem., Int. Ed.* **2006**, *45*, 38−68.

(3) Gin, D.; Pecinovsky, C.; Bara, J.; Kerr, R. In *Liquid Crystalline Functional Assemblies and Their Supramolecular Structures*; Kato, T., Ed.; Structure and Bonding; Springer: Berlin, 2008; Vol. *128*, pp 181−222.

(4) Lynch, M., Lynch, M., Spicer, P., Eds.; *Bicontinuous Liquid Crystals*; Surfactant Science Series; CRC Press, 2005; pp 1−512.

(5) Menger, F. M.; Keiper, J. S. Gemini Surfactants. *Angew. Chem., Int. Ed.* **2000**, *39*, 1906−1920.

(6) Menger, F. M.; Littau, C. A. Gemini Surfactants: A New Class of Self-Assembling Molecules. *J. Am. Chem. Soc.* **1993**, *115*, 10083−10090.

(7) Zana, R. Gemini (Dimeric) Surfactants. *Curr. Opin. Colloid Interface Sci.* **1996**, *1*, 566−571.

(8) Zana, R. Dimeric (Gemini) Surfactants: Effect of the Spacer Group on the Association Behavior in Aqueous Solution. *J. Colloid Interface Sci.* **2002**, *248*, 203−220.

(9) Sorenson, G. P.; Coppage, K. L.; Mahanthappa, M. K. Unusually Stable Aqueous Lyotropic Gyroid Phases from Gemini Dicarboxylate Surfactants. *J. Am. Chem. Soc.* **2011**, *133*, 14928−14931.

(10) Perroni, D. V.; Baez-Cotto, C. M.; Sorenson, G. P.; Mahanthappa, M. K. Linker Length-Dependent Control of Gemini Surfactant Aqueous Lyotropic Gyroid Phase Stability. *J. Phys. Chem. Lett.* **2015**, *6*, 993−998.

DOI: 10.1021/acs.jpcb.6b06882
J. Phys. Chem. B 2017, 121, 565−576

(11) Gin, D. L.; Bara, J. E.; Noble, R. D.; Elliott, B. J. Polymerized Lyotropic Liquid Crystal Assemblies for Membrane Applications. *Macromol. Rapid Commun.* **2008**, *29*, 367−389.
(12) Hatakeyama, E. S.; Wiesenauer, B. R.; Gabriel, C. J.; Noble, R. D.; Gin, D. L. Nanoporous, Bicontinuous Cubic Lyotropic Liquid Crystal Networks via Polymerizable Gemini Ammonium Surfactants. *Chem. Mater.* **2010**, *22*, 4525−4527.
(13) Gin, D.; Lu, X.; Nemade, P.; Pecinovsky, C.; Xu, Y.; Zhou, M. Recent Advances in the Design of Polymerizable Lyotropic Liquid-Crystal Assemblies for Heterogeneous Catalysis and Selective Separations. *Adv. Funct. Mater.* **2006**, *16*, 865−878.
(14) Miller, S. A.; Kim, E.; Gray, D. H.; Gin, D. L. Heterogeneous Catalysis with Cross-Linked Lyotropic Liquid Crystal Assemblies: Organic Analogues to Zeolites and Mesoporous Sieves. *Angew. Chem., Int. Ed.* **1999**, *38*, 3021−3026.
(15) Xu, Y.; Gu, W.; Gin, D. L. Heterogeneous Catalysis Using a Nanostructured Solid Acid Resin Based on Lyotropic Liquid Crystals. *J. Am. Chem. Soc.* **2004**, *126*, 1616−1617.
(16) Kerr, R. L.; Miller, S. A.; Shoemaker, R. K.; Elliott, B. J.; Gin, D. L. New Type of Li Ion Conductor with 3D Interconnected Nanopores via Polymerization of a Liquid Organic Electrolyte-Filled Lyotropic Liquid-Crystal Assembly. *J. Am. Chem. Soc.* **2009**, *131*, 15972−15973.
(17) Spicer, P. T. Progress in Liquid Crystalline Dispersions: Cubosomes. *Curr. Opin. Colloid Interface Sci.* **2005**, *10*, 274−279.
(18) Leal, C.; Bouxsein, N. F.; Ewert, K. K.; Safinya, C. R. Highly Efficient Gene Silencing Activity of siRNA Embedded in a Nanostructured Gyroid Cubic Lipid Matrix. *J. Am. Chem. Soc.* **2010**, *132*, 16841−16847.
(19) Buhler, E.; Mendes, E.; Boltenhagen, P.; Munch, J. P.; Zana, R.; Candau, S. J. Phase Behavior of Aqueous Solutions of a Dimeric Surfactant. *Langmuir* **1997**, *13*, 3096−3102.
(20) In, M.; Zana, R. Phase Behavior of Gemini Surfactants. *J. Dispersion Sci. Technol.* **2007**, *28*, 143−154.
(21) Menger, F. M.; Peresypkin, A. V. A Combinatorially-Derived Structural Phase Diagram for 42 Zwitterionic Geminis. *J. Am. Chem. Soc.* **2001**, *123*, 5614−5615.
(22) Zhou, M.; Nemade, P. R.; Lu, X.; Zeng, X.; Hatakeyama, E. S.; Noble, R. D.; Gin, D. L. New Type of Membrane Material for Water Desalination Based on a Cross-Linked Bicontinuous Cubic Lyotropic Liquid Crystal Assembly. *J. Am. Chem. Soc.* **2007**, *129*, 9574−9575.
(23) Pindzola, B. A.; Jin, J.; Gin, D. L. Cross-Linked Normal Hexagonal and Bicontinuous Cubic Assemblies via Polymerizable Gemini Amphiphiles. *J. Am. Chem. Soc.* **2003**, *125*, 2940−2949.
(24) Gin, D. L.; Bara, J. E.; Noble, R. D.; Zheng, X. Surfactants and Polymerizable Surfactants Based on Room-temperature Ionic Liquids That Form Lyotropic Liquid Crystal Phases With Water and Room-temperature Ionic Liquids. U.S. Patent 7,931,824, 2011.
(25) Mondal, J.; Mahanthappa, M. K.; Yethiraj, A. Self-Assembly of Gemini Surfactants: A Computer Simulation Study. *J. Phys. Chem. B* **2013**, *117*, 4254−4262.
(26) Zhu, Y.-P.; Masuyama, A.; Kobata, Y.; Nakatsuji, Y.; Okahara, M.; Rose, M. J. Double-Chain Surfactants with Two Carboxylate Groups and Their Relation to Similar Double-Chain Compounds. *J. Colloid Interface Sci.* **1993**, *158*, 40−45.
(27) Hordyjewicz-Baran, Z.; Woch, J.; Kuliszewska, E.; Zimoch, J.; Libera, M.; Dworak, A.; Trzebicka, B. Aggregation Behavior of Anionic Sulfonate Gemini Surfactants with Dodecylphenyl Tails. *Colloids Surf., A* **2015**, *484*, 336−344.
(28) Dreja, M.; Pyckhout-Hintzen, W.; Mays, H.; Tieke, B. Cationic Gemini Surfactants with Oligo(oxyethylene) Spacer Groups and Their Use in the Polymerization of Styrene in Ternary Microemulsion. *Langmuir* **1999**, *15*, 391−399.
(29) Liu, X.-P.; Feng, J.; Zhang, L.; Gong, Q.-T.; Zhao, S.; Yu, J.-Y. Synthesis and Properties of a Novel Class of Anionic Gemini Surfactants with Polyoxyethylene Spacers. *Colloids Surf., A* **2010**, *362*, 39−46.
(30) De, S.; Aswal, V. K.; Goyal, P. S.; Bhattacharya, S. Role of Spacer Chain Length in Dimeric Micellar Organization. Small Angle Neutron Scattering and Fluorescence Studies. *J. Phys. Chem.* **1996**, *100*, 11664−11671.
(31) Li, R.; Yan, F.; Zhang, J.; Xu, C.; Wang, J. The Self-Assembly Properties of a Series of Polymerizable Cationic Gemini Surfactants: Effect of the Acryloxyl Group. *Colloids Surf., A* **2014**, *444*, 276−282.
(32) Li, Y.; Li, P.; Wang, J.; Wang, Y.; Yan, H.; Thomas, R. K. Odd/Even Effect in the Chain Length on the Enthalpy of Micellization of Gemini Surfactants in Aqueous Solution. *Langmuir* **2005**, *21*, 6703−6706.
(33) Yoshimura, T.; Esumi, K. Synthesis and Surface Properties of Anionic Gemini Surfactants with Amide Groups. *J. Colloid Interface Sci.* **2004**, *276*, 231−238.
(34) Gao, B.; Sharma, M. M. A Family of Alkyl Sulfate Gemini Surfactants. 1. Characterization of Surface Properties. *J. Colloid Interface Sci.* **2013**, *404*, 80−84.
(35) Martin, V. I.; Rodriguez, A.; Lopez-Cornejo, P.; Luisa Moya, M. Role of the Spacer in the Non Ideal Behavior of Alkanedyil-α,ω-bis(dodecyldimethylammonium) Bromide-MEGA10 Binary Mixtures. *Colloids Surf., A* **2013**, *418*, 139−146.
(36) Ueno, M.; Takasawa, Y.; Miyashige, H.; Tabata, Y.; Meguro, K. Effects of Alkyl Chain Length on Surface and Micellar Properties of Octaethyleneglycol-n Alkyl Ethers. *Colloid Polym. Sci.* **1981**, *259*, 761−766.
(37) Cuy, E. J. The Electronic Constitution of Normal Carbon Chain Compounds, Saturated and Unsaturated. *J. Am. Chem. Soc.* **1920**, *42*, 503−514.
(38) Lunkenheimer, K.; Haage, K.; Hirte, R. Novel Results on the Adsorption Properties of n-Alkyldimethylphosphine Oxides at the Air/Water Interface. *Langmuir* **1999**, *15*, 1052−1058.
(39) Varghese, N.; Shetye, G. S.; Yang, S.; Wilkens, S.; Smith, R. P.; Luk, Y.-Y. The Ability of Single-Chain Surfactants to Emulsify an Aqueous-Based Liquid Crystal Oscillates with Odd-Even Parity of Alkyl-Chain Length. *J. Colloid Interface Sci.* **2013**, *412*, 95−99.
(40) Pronk, S.; Páll, S.; Schulz, R.; Larsson, P.; Bjelkmar, P.; Apostolov, R.; Shirts, M. R.; Smith, J. C.; Kasson, P. M.; van der Spoel, D.; et al. GROMACS 4.5: A High-throughput and Highly Parallel Open Source Molecular Simulation Toolkit. *Bioinformatics* **2013**, *29*, 845−854.
(41) Schuler, L. D.; Daura, X.; van Gunsteren, W. F. An Improved GROMOS96 Force Field for Aliphatic Hydrocarbons in the Condensed Phase. *J. Comput. Chem.* **2001**, *22*, 1205−1218.
(42) Berendsen, H.; Postma, J.; van Gunsteren, W.; Hermans, J. In *Intermolecular Forces*; Pullman, B., Pullman, B., Eds.; The Jerusalem Symposia on Quantum Chemistry and Biochemistry; Reidel: Dordrecht, Holland, 1981; Vol. *14*, pp 331−342.
(43) Essmann, U.; Perera, L.; Berkowitz, M. L.; Darden, T.; Lee, H.; Pedersen, L. G. A Smooth Particle Mesh Ewald Method. *J. Chem. Phys.* **1995**, *103*, 8577−8593.
(44) Miyamoto, S.; Kollman, P. A. Settle: An Analytical Version of the SHAKE and RATTLE Algorithm for Rigid Water Models. *J. Comput. Chem.* **1992**, *13*, 952−962.
(45) Berendsen, H. J. C.; Postma, J. P. M.; van Gunsteren, W. F.; DiNola, A.; Haak, J. R. Molecular Dynamics With Coupling to an External Bath. *J. Chem. Phys.* **1984**, *81*, 3684−3690.
(46) McDaniel, J. G.; Mantha, S.; Yethiraj, A. Dynamics of Water in Gemini Surfactant-Based Lyotropic Liquid Crystals. *J. Phys. Chem. B* **2016**, *120*, 10860−10868.
(47) Rancon, Y.; Charvolin, J. Fluctuations and phase transformations in a lyotropic liquid crystal. *J. Phys. Chem.* **1988**, *92*, 6339−6344.
(48) Bates, F. S.; Rosedale, J. H.; Fredrickson, G. H. Fluctuation Effects in a Symmetric Diblock Copolymer Near the Order-disorder Transition. *J. Chem. Phys.* **1990**, *92*, 6255−6270.
(49) Tristram-Nagle, S.; Nagle, J. F. Lipid Bilayers: Thermodynamics, Structure, Fluctuations, and Interactions. *Chem. Phys. Lipids* **2004**, *127*, 3−14.
(50) Matsen, M. W. Cylinder ↔ Gyroid Epitaxial Transitions in Complex Polymeric Liquids. *Phys. Rev. Lett.* **1998**, *80*, 4470−4473.

DOI: 10.1021/acs.jpcb.6b06882
J. Phys. Chem. B 2017, 121, 565−576

(51) Fredrickson, G. H.; Helfand, E. Fluctuation Effects in the Theory of Microphase Separation in Block Copolymers. *J. Chem. Phys.* **1987**, *87*, 697−705.
(52) Liu, C. K.; Warr, G. G. Self-Assembly of Didodecyldimethylammonium Surfactants Modulated by Multivalent, Hydrolyzable Counterions. *Langmuir* **2015**, *31*, 2936−2945.
(53) Brotons, G.; Dubois, M.; Belloni, L.; Grillo, I.; Narayanan, T.; Zemb, T. The Role of Counterions on the Elasticity of Highly Charged Lamellar Phases: A Small-angle X-ray and Neutron-scattering Determination. *J. Chem. Phys.* **2005**, *123*, No. 024704.
(54) Liu, C. K.; Warr, G. G. Hexagonal Closest-packed Spheres Liquid Crystalline Phases Stabilised by Strongly Hydrated Counterions. *Soft Matter* **2014**, *10*, 83−87.

DOI: 10.1021/acs.jpcb.6b06882
J. Phys. Chem. B 2017, 121, 565−576